Acta Cryst. (1980). A**36**, 104–116

Secondary Reflections in Multiple Scattering and their Interference

BY H. JAGODZINSKI

Institut für Kristallographie und Mineralogie der Ludwig-Maximilians-Universität, Theresienstrasse 41, 80000 *München* 2, *Federal Republic of Germany*

(*Received* 28 *May* 1979; *accepted* 6 *August* 1979)

Abstract

A focusing monochromatic X-ray single-crystal technique (Noromosic technique) is applied to investigate shape and interference phenomena of multiply scattered X-ray reflections. It is shown that this technique allows for rapid elimination of spurious 'peaks' caused by coherent or incoherent multiple-scattering processes (*Umweganregung*). No rotation of the crystal around the reciprocal vector in question is necessary. Furthermore, it is shown that phase determination can be done in principle if two secondary reflected beams are brought to interference within the crystal. This may generally be realized in the *n*-beam case of diffraction ($n \geq 4$) by changing the wavelength or the lattice geometry. The method is applied to α-phenazine, $C_{12}H_8N_2$, where four- and six-beam cases occur accidentally without a variation of the wavelength. It is shown that phase determination is possible even in such cases where a certain mosaic spread of the crystal is unavoidable.

1. Introduction

Accurate structure determination strongly depends on reliable corrections of $|F(hkl)|$. It is well known that the correction for extinction causes difficulties in multiple scattering, which generally occurs if more than one reflection is excited simultaneously by the primary beam, although in principle this problem may be solved experimentally by rotating the crystal around the normal of the reflecting plane (*hkl*). In order to determine precise electron densities, the phases of the reflections – even of the weak ones – must be known accurately; this specifically holds for non-centrosymmetric crystals. It will be shown in the following that all these difficulties may be overcome in part by applying a diffraction technique that has already been published (Jagodzinski, 1968). This method provides a means for rapid correction of measured peak intensities caused by multiple scattering of secondary reflections. An experimental method for phase determination of strong and weak $F(hkl)$ is also possible.

In a preliminary communication the author has published some of the most important results (Jagodzinski, 1978). It will be shown in this paper that the method used here is applicable even to imperfect crystals. Recently, Post (1979) has published some experimental results on interference in the so-called three-beam case, using perfect Ge and α-Al_2O_3 crystals. A different experiment on interference in the three-beam case has been published by Collela (1974), but the conclusions drawn from it, and the experimental method were criticized by Post (1975), and the author agrees that the experiment was not well suited to phase determination. It will be shown in the following article that the four-beam case is best suited for a successful determination of phases; unfortunately, an X-ray source with intense white radiation is needed unless the four-beam case can be realized by accidental geometrical symmetries of the reciprocal lattice, which need not be symmetries of the crystal. The theory of the four-beam case has been developed by Ewald & Héno (1968; Héno & Ewald, 1968), unfortunately, it cannot be applied to the diffraction geometry used in an experiment which is sensitive to the boundary conditions introduced. Therefore, an extension of the theory is needed in order to give a full interpretation of the interference patterns observed. In spite of the fact that the final solution of this diffraction problem can only be given with the aid of the dynamical theory of scattering, a qualitative approach to the interpretation of the diffraction pattern will be given here by using pseudo-kinematic arguments, but keeping in mind that this kind of approach can be no more than a first approximation to the final dynamical solution.

2. Experimental method

All experiments have been done with strictly monochromatic Cu $K\alpha_1$ radiation produced with the aid of a bent quartz single-crystal. Generally, we used large single-crystals as samples in order to observe the propagating waves within the crystal. The experimental X-ray equipment was an evacuable oscillation camera; the focusing principle and its resolution power has been

0567-7394/80/010104-13$01.00

described previously by the author (Jagodzinski, 1968).

Fig. 1 shows the diffraction geometry realized in our experiment. According to Fig. 1(*a*) each volume element of the big crystal receives a small angle of aperture in the vertical direction, as determined by the monochromator ($\sim 1'$, this angle is mainly due to the inaccuracy of the wavelength $\Delta\lambda$), but a rather large one ($\sim 1°$) in the horizontal direction. Since strictly monochromatic radiation (λ_0) is used, only parallel beams within the horizontal angle of aperture are effective for Bragg reflections of a standing crystal (Fig. 1*a*). All volume elements lying on a vertical line (Fig. 1*b*) continuously reflect λ_0 by rotating the crystal. The full and the broken lines in Fig. 1(*b*) indicate the angular range of diffraction given by the angle of aperture.

The focusing condition of reflections scattered by the incident beam $\mathbf{s}_0$ in the equatorial plane is shown in Fig. 2. Since diffraction may be described by the corresponding Kossel cones, reflection takes place for each volume element of the crystal regardless of its height, and the reflection is focused in the zero layer line on the film. The line width in the vertical direction of reflections in the zero layer line is mainly determined by the monochromator. In the horizontal direction the line width is given by the width of the beam (Fig. 1*a*) and the horizontal angle of aperture (Fig. 1*b*), which may be calculated from the effective length of the line focus of the X-ray tube as limited by *B* (Fig. 1*b*). This is valid as long as the size of the crystal does not impose another limitation. In our experiment the size of the crystal was large when compared with the dimensions of the X-ray beam. Obviously, this method applied to a standing crystal is equivalent to an oscillation of the crystal by an angle equal to the horizontal aperture in the parallel-beam method (Noromosic technique). The accuracy and the formal oscillation angle is determined by the horizontal angle of aperture, while the vertical one does not have any influence on the resolution power.

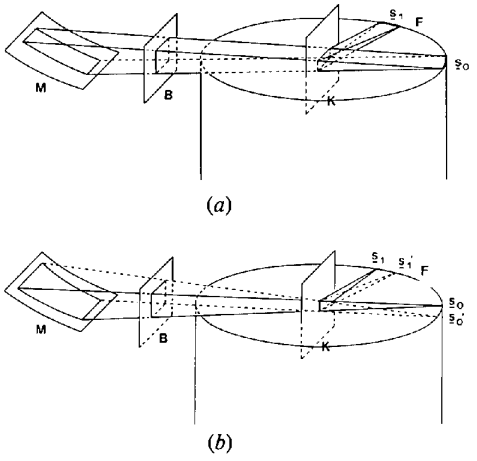

Fig. 1. Diffraction geometry in the Noromosic technique. (*a*) The line focus of the monochromator *M* is placed horizontally on the film *F*. The vertical angle of aperture for each volume element is small. A plane section through the crystal is shown only. (*b*) A large horizontal angle of aperture is available, but a small part only is effective for Bragg scattering. The full and broken lines of the beams represent the two extreme positions for Bragg reflection in a vertical row of volume elements.

Let us now assume that two reflections are scattered simultaneously (three-beam case), the diffraction condition may then be best described by two crossing Kossel cones. Consequently, the angle of aperture effective for multiple scattering (secondary reflections) is small, while the primary reflections may take up the larger angle of aperture corresponding to their individual Kossel cones. This is shown in Fig. 3, where it has been tacitly assumed that the two Kossel cones meet precisely in the equatorial plane.

The Ewald conditions valid in this case are

$$\mathbf{h}_1 = (\mathbf{s}_1 - \mathbf{s}_0)/\lambda, \quad \mathbf{h}_2 = (\mathbf{s}_2 - \mathbf{s}_0)/\lambda \qquad (1a)$$

(primary reflections), and it may be seen that

$$\mathbf{h}_1 - \mathbf{h}_2 = (\mathbf{s}_1 - \mathbf{s}_2)/\lambda, \quad \mathbf{h}_2 - \mathbf{h}_1 = (\mathbf{s}_2 - \mathbf{s}_1)/\lambda \qquad (1b)$$

(secondary reflections) are satisfied also. Equations (1*a*) and (1*b*) mean that the two primary reflections $\mathbf{s}_1$ and $\mathbf{s}_2$ excited by $\mathbf{s}_0$ generate secondary reflections scattered in the directions $\mathbf{s}_2$ and $\mathbf{s}_1$, respectively. As

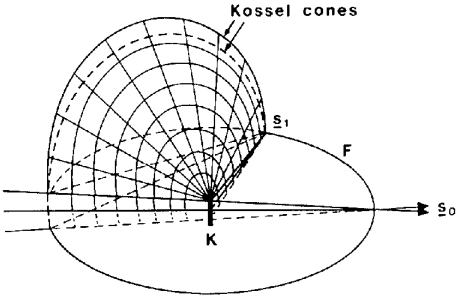

Fig. 2. Explanation of the focusing condition with the aid of Kossel cones. $\mathbf{s}_0$ and $\mathbf{s}_1$ are the directions of the incident and reflected beams, respectively.

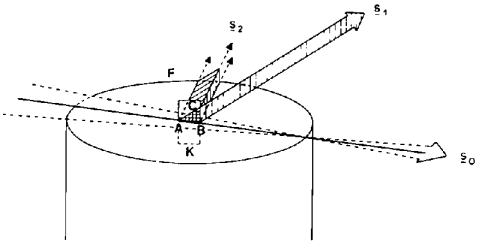

Fig. 3. In the case of multiple diffraction a secondary reflection can be generated in a small range of the angle of aperture only. The crossing of two Kossel cones is represented by the central line *AB* showing the effective part of $\mathbf{s}_0$, which generates a primary reflection ($\mathbf{s}_1$) capable of producing a secondary reflection ($\mathbf{s}_2$). The cross-hatched area *ABC* represents the volume irradiated by $\mathbf{s}_1$.

shown in Fig. 3, this condition is satisfied only for a small part of the crystal (line AB). Now, the complete explanation of multiple scattering is given by remembering that the primary reflection $\mathbf{s}_1$ (and $\mathbf{s}_2$!) propagates according to its Bormann fan, generally describing the propagation of wave fields in the interior of the crystal. Therefore, $\mathbf{s}_1$ covers a much larger volume (represented by the area ABC in Fig. 3) than the part AB of the primary beam, effective for multiple diffraction. It is assumed here that $\mathbf{s}_1$ may well be described by a plane wave, then the whole volume irradiated by $\mathbf{s}_1$ causes the secondary reflection $\mathbf{s}_2$ shown in Fig. 3 (the primary reflection $\mathbf{s}_2$ generated by $\mathbf{s}_0$ is not shown in this figure). Let us now refer to the case relevant to this paper, where the experimental geometry is such that the center of the primary beam is in the plane of symmetry of a monoclinic crystal. Here the three-beam case is realized anyway by the symmetry condition. Both $F(hkl)$ and $F(h\bar{k}l)$ are reflected simultaneously, if the crystal is oriented parallel to [010] of the oscillation camera (Fig. 1) and $k \neq 0$ (non-equatorial reflection). The diffraction geometry for secondary reflections may then be represented as shown in Fig. 4.

Although $\mathbf{s}_1$ and $\mathbf{s}_2$ are generated by a larger angle of aperture, only a small angular part of $\mathbf{s}_0$ generates the appropriate parts of beams $\mathbf{s}_1$ and $\mathbf{s}_2$, effective for secondary reflections. Furthermore, it should be noted that the part of $\mathbf{s}_0$ falling outside the plane of symmetry may generate single primary beams $\mathbf{s}_1$ or $\mathbf{s}_2$ only. Consequently, extinction should be appreciably higher for the partial beam in the plane of symmetry. The shape of the volume irradiated by the two primary beams $\mathbf{s}_1$ and $\mathbf{s}_2$ for a rectangular crystal block is a fat-type 'arrow', spearheading at its entrance (Laue case) into the crystal. It changes slightly when the incident beam $\mathbf{s}_0$ is inclined to the frontal surface of the block. Now it may easily be seen why interference may not be observed in this case; as long as the primary beam is much stronger than the secondary one (and this was true in our experiment), the intensity of the primary beam, although generated by a smaller volume, prevents the observation of interference effects. There would be a definite chance if one of the two primary scattered reflections had a much lower intensity. This cannot be realized in symmetrically equivalent reflections. The situation changes drastically when a third reflection in the plane of symmetry $F(h0l)$ meets the Ewald sphere simultaneously. In order to facilitate the understanding of the diffraction phenomena, the band of the incident beam $\mathbf{s}_0$ is represented by a single line only in Fig. 5.

Each of the directions $\mathbf{s}_0$, $\mathbf{s}_1$, $\mathbf{s}_2$, $\mathbf{s}_3$ now contains three contributions, one primary reflection (generated by $\mathbf{s}_0$) and two secondary ones, excited by the remaining two of the three primary reflections $\mathbf{s}_1$, $\mathbf{s}_2$, $\mathbf{s}_3$. In Fig. 5 this situation is shown when $\mathbf{s}_3$ falls into the zero layer line. The whole diffraction pattern may now be constructed:

(*a*) by superimposing the various parts of the band effective for multiple scattering according to Fig. 4;

(*b*) by remembering that the remaining part of the primary beam $\mathbf{s}_0$ generates the primary reflections in the zero layer line as well, where it is fully focused.

A typical diffraction pattern of this type is shown in Fig. 7, which will be discussed below. The picture of the two primary reflections, $\mathbf{s}_1$ and $\mathbf{s}_2$, is projected onto the film by two secondary reflections generated by $\mathbf{s}_1$ and $\mathbf{s}_2$ in the direction $\mathbf{s}_3$. Interference would be possible in that part of the diffraction pattern where the two wings of $\mathbf{s}_1$ and $\mathbf{s}_2$ overlap. Unfortunately, here, the primary reflection, the intensity of which is even more increased by the focusing effect, is strongly overexposed. Although the latter effect may be reduced by diminishing the vertical angle of aperture (compare with Fig. 1), it remains strong as long as the $F(hkl)$ in question is not extremely small (*e.g.* accidental or systematic absences).

The shape of the reflection in Fig. 7 clearly shows that the contribution of secondary reflections to the primary one may well be separated by taking a photometer record of the whole reflection vertical to the sharp primary peak. Apparently this procedure may also be applied to diffractometers of any kind, if the

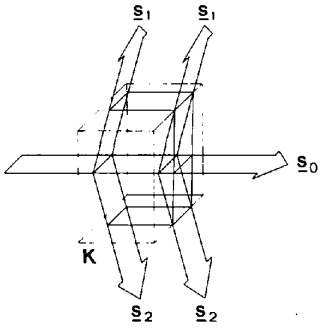

Fig. 4. The three-beam case in our diffraction technique. Only the primary reflections $\mathbf{s}_1$, $\mathbf{s}_2$ are shown. Secondary reflections are scattered in both directions, but the whole volume irradiated by the two primary reflections contributes to the secondary reflections.

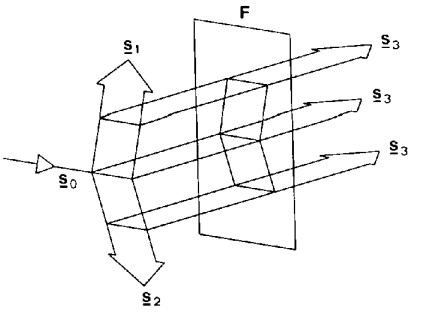

Fig. 5. The geometry of the four-beam case and the explanation of the shape of secondary reflections. The line of $\mathbf{s}_0$ represents a 'band'. Correspondingly, the other directions of diffraction have to be supplemented.

Noromosic technique is extended to diffractometers. It should be pointed out here that multiple scattering takes place more frequently than generally assumed, and high-resolution techniques using small angles of aperture enhance the effect of secondary reflections considerably. Therefore, the present diffractometer techniques are not optimal for a reliable record of weak reflections. The Noromosic technique has the advantage of admitting large angles of aperture without diminishing the high resolution power and without increasing the danger of a completely wrong intensity measurement. On the other hand, crystals of a minimum size are needed in order to rule out the secondary reflections from the primary ones. Since the width of reflections may be reduced to less than 0·05 mm, a crystal size of approximately 0·2 mm would be sufficient to carry out this procedure. Since crystals of this size are very often available, the only limitation could be a high absorption coefficient. Finally, the geometry of the six-beam case, which is particularly important for α-phenazine, is shown in Fig. 6, which will be discussed below.

3. Interference patterns in α-phenazine

The interference experiments, as described in this paper, were initiated by a collaboration between Professor Hausser and Mr Zimmermann, Heidelberg. Schuch, Stehlik & Hausser (1971) found very strange behavior in certain single crystals of α-phenazine, $C_{12}H_8N_2$, in their experiments on optical nuclear polarization, which seemed to be correlated with an unknown anomaly of the structure. Crystals of different quality exhibited a change of their spectra as a function of their orientation of the magnetic field. X-ray investigation revealed a correlation of this effect with the mosaic spread of the crystals (Hausser, 1979). Fortunately, many crystals with different mosaic spread were synthesized by growing them from the vapour phase or from the melt; the latter crystals generally were of lower quality. Although crystals of a considerable size were used (plates 1–2 mm in length and 0·5–1 mm thick), the penetration of the Cu $K\alpha_1$ radiation was quite satisfactory, such that the intensity of the primary beam was reduced to no more than 50%. The intensities of the strongest primary and secondary reflections differed by about three orders of magnitude (10^3). This could be checked by estimating the exposure time of the primary beam and the strongest primary and secondary reflections. Since the cross section for absorption in α-phenazine is lower than the cross section for coherent elastic scattering, the same experimental conditions may not be realized for Si and Ge crystals predominantly used in former experiments. For this reason we may conclude that the interference phenomena observed by us are not caused by the well-known enhanced Borrmann effect, as reported by Huang & Post (1973) and Kshevetsky & Mikhailyuk (1976). Naturally, the diffraction conditions valid in the interior of α-phenazine have to be determined by using the dispersion surfaces of the dynamical theory of diffraction. Fortunately, the refraction index $1-\Delta n$ is very near to unity in the case of α-phenazine where $\Delta n \simeq 3 \times 10^{-5}$. Since the angular resolution power of the camera is not very large (the diffraction conditions given by the crystal excepted), all angular corrections may be neglected.

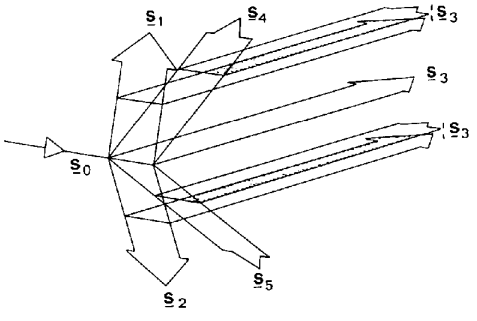

Fig. 6. Overlapping areas of secondary reflections in the six-beam case of multiple scattering. Compare with Figs. 4 and 5.

α-Phenazine crystallizes in space group $P2_1/a$, and its structure has been determined and discussed by Herbstein & Schmidt (1955*a*,*b*). Hirshfeld (1955) reported on the unusual forbidden reflection 500, but the conclusions drawn regarding phase determination were unsatisfactory. Since the space group demands the extinction rule

$$F(h0l) = 0 \quad \text{if } h = \text{odd},$$

there are many systematic absences in the zero layer line of a rotation or oscillation photograph with [010] as rotation axis. At the beginning of our experiments we noticed that the forbidden 500 reflection was very sensitive to the quality of the crystal. Consequently, we concluded that the unusual multiple diffraction is an effect of the mosaic spread of the crystal, which here shall be called 'incoherent multiple diffraction'. Systematic studies of absent reflections (*h*0*l*) with the aid of the Noromosic technique revealed that a lot of forbidden reflections can be observed. But a careful check of the geometry of such accidental coincidences revealed that, once the condition of the coherent or incoherent multiple scattering is realized accidentally for a crystal of low symmetry, similar coincidences of reflections may occur very frequently for other settings of the crystal using the same wavelength. A more detailed explanation of this fact will be given below with the aid of coincidences caused by accidental geometrical proportions of α-phenazine.

Multiple diffraction has been observed for seven (*h*0*l*) reflections, five of them belonging to the sys-

tematically absent ones as described by the extinction rule of the space group $P2_1/a$ mentioned above.

Table 1 gives the angular positions for the crystal $K11$, which was not too perfect. Obviously these reflections do not appear simultaneously, although they are observed in the very narrow angular range of 3° approximately. Multiple diffraction in the four-beam case takes place when four points of the reciprocal lattice meet the Ewald sphere simultaneously. This can generally be realized by changing the radius $(1/\lambda)$ of the Ewald sphere. If these four reciprocal-lattice points lie in the same reciprocal plane, they belong to the same zone $[uvw]$. The intersection of the common reciprocal plane and the Ewald sphere is a circle. Therefore, it is a necessary prerequisite that they lie on the circumference of a common circle. Consequently, it may be concluded that the coincidence takes place for all wavelengths as long as the radius of the said circle is smaller than that of the Ewald sphere. This particular case is realized in α-phenazine twice. If the four reciprocal-lattice points do not belong to the same zone, the wavelength has to be varied in order to meet the diffraction conditions simultaneously as already mentioned above.

In α-phenazine

$$000,\ 421,\ 42\bar{1},\ 802,\ (\text{zone } [10\bar{4}])$$

are almost on the same circle, and the same is true for the two equivalent groups

$$\left.\begin{matrix}000,\ 310,\ 3\bar{1}0,\ 210,\ 2\bar{1}0,\ 500\\ 000,\ \bar{3}10,\ \bar{3}\bar{1}0,\ \bar{2}10,\ \bar{2}\bar{1}0,\ \bar{5}00\end{matrix}\right\}\ \text{zone } [001].$$

But it should be emphasized that this coincidence is not due to the symmetry of the crystal. As we will show below, there is indeed a big difference in the character of multiple diffraction of these two groups. Now it may easily be shown by considering the lattice geometry that non-planar coincidences are possible on the same Ewald sphere for other reciprocal-lattice points of the same lattice. For this reason, α-phenazine represents a very fortunate case for studying multiple-diffraction phenomena without changing the wavelength of X-rays. In our experiment Cu $K\alpha_1$ radiation has been used. Naturally it is most probable that the circle or sphere condition for reciprocal-lattice points is not satisfied exactly. Since the propagation of waves in the interior of the crystal has to be described by their dispersion surfaces rather than the Ewald sphere, it does not seem worthwhile to have a more detailed discussion on possible deviations using the kinematic approximation. New, accurate experiments have to be done by changing the wavelength or the lattice geometry (*e.g.* by thermal expansion) in order to meet the optimal conditions for exciting waves. Curious interference phenomena have already been reported by Renninger (1978) for diffraction angles deviating from the Bragg condition in the two-beam case, and there is no doubt that similar effects have to be expected in our experiments. All crystals used here were plates parallel to (001) of approximately 0·5–1 mm thickness, the other dimensions were 2–4 mm. Consequently, the primary beam was 'bathed' by the crystal. But it should be pointed out that in spite of its large size the crystal was more or less transparent, since no shadows of the diffuse background due to absorption (plates!) could be observed; obviously the absorption coefficient is very small ($\mu \simeq 6{\cdot}5$) and we should remember, that μ is much larger (by a factor of 25) in the case of Si.

Table 1. *Positions of secondary reflection observed in* $K11$

The cross (×) indicates the optimal position of the secondary reflection. The same relative angles are observed in the other crystals discussed in this paper.

Angle (°)	$\bar{5}00$	304	$\bar{1}\bar{1}$,0,2	Angle (°)	$\bar{7}03$	500	804	802
312·5	|			276·5	| ×	|		
313	||			277	| ×	|| ×		
313·5	|| ×	|		277·5	|	|| ×	|	
314	||	| ×					×	
314·5	|	|		278·5			|	||
315			|| ×					|| ×

Most of the multiple diffractions belong to the Laue case, except 804 and 304, but the primary reflection is absent in the case of 304. Now the angle ψ' at the point of the arrowhead may be determined according to the equation

$$\tan \psi'/2 = \tan \psi/\sin(\varphi_2 - \varphi_1), \qquad (2)$$

this angle is given in Table 2 and compared with the corresponding angles observed experimentally. Table 2 also contains the kinematic reflection intensities of primarily and secondarily reflecting planes. By assum-

Table 2 gives the necessary information on the directions of the primary beam (in reciprocal coordinates $x^*\,\mathbf{a}^* + z^*\,\mathbf{b}^*$ of the center of the Ewald sphere, opposite direction to the incident beam), and the angle ψ' discussed below. Table 2(*b*) shows that the second group occurs at a nearly vertical incidence of the (001) surface of the crystal (x^* is small), while 2(*a*) indicates an inclined angle. As may be concluded from the angles given in Table 1, this angle of inclination amounts to approximately 37°. Since all multiply scattered reflections occur in a very small angular range the reader gets a clear idea of the beam geometry. The diffraction angle is determined by the layer-line angle ψ and the azimuthal angle φ. Table 3 shows, for primary reflections, whether the beams belong to the Laue (*L*) or Bragg (*B*) case, and gives their azimuthal scattering angles.

Table 2. *Position of the center of the Ewald sphere according to the Bragg condition given in reciprocal coordinates x^*, z^* (x^* **a*** + z^* **c***), and angle ψ' at the point of the arrow*

Estimated intensities are listed as follows: *vvs* = extremely strong; *vs* = very strong; *s* = strong; *m* = medium; *vw* = very weak; *w* = weak.

(*a*) Reflection group associated with $\bar{5}00$

Strong primary reflection	$\bar{2}10$ *vs* −5·21; 4·39	$\bar{3}10$ *vvs* −5·20; 4·37	211 *vs* −5·26; 4·37	Observed angle ψ', *cf.* equation (2)
Extinguished primary reflection				
$\bar{5}00$ −5·20; 4·38	$3\bar{1}0$ *vvs* 83°	$2\bar{1}0$ *vs* 105°	$\bar{7}1\bar{1}$ *w* 41°	ψ' fluctuating ~90°
304 −5·28; 4·37	$5\bar{1}4$ *m* 36°	$6\bar{1}4$ *w* 36°	$1\bar{1}3$ *m–s* 51°	o.k. 38–40°
$\bar{1}\bar{1}$,0,2 −5·44; 4·33	$9\bar{1}2$ *w* 39°	$8\bar{1}2$ *m* 42°	$\bar{1}\bar{3}$,$\bar{1}$,1 *vw* 36°	o.k. 44°

(*b*) Reflection group associated with 500

Strong primary reflection	210 *vs* −0·19; 4·38	310 *vvs* −0·19; 4·37	421 *vs* −0·39; 4·41	Observed angle ψ', *cf.* equation (2)
Extinguished or weak primary reflection				
500 −0·20; 4·38	$3\bar{1}0$ *vvs* 83°	$2\bar{1}0$ *vs* 105°	$12\bar{1}$ *w* 179°	fluctuating ~108–110°
$\bar{7}03$ −0·115; 4·37	$9\bar{1}3$ *w* 38°	$\bar{1}\bar{0}$,1,3 *m* 37°	$\bar{1}\bar{1}$,2,2 *vw* 75·1°	o.k. 37·5°
804 −0·30; 4·40	$6\bar{1}4$ *w* 36°	$5\bar{1}4$ *m* 36°	$42\bar{3}$ *w* 82°	o.k. 35°
802 −0·39; 4·41	$6\bar{1}2$ *vw* 40°	$5\bar{1}2$ *m* 43°	$42\bar{1}$ 104°	o.k. 99°

Table 3. *Characterization of the diffraction geometry of primary reflections*

L = Laue case, B = Bragg case, φ_l = azimuthal angle.

Indices	L, B	φ_l (°)	Indices	L, B	φ_l (°)
310	L	+21	$\bar{3}10$	L	−21
210	L	+14	$\bar{2}10$	L	−14
421	L	+39	211	L	+23
500	L	+35	$\bar{5}00$	L	−35
802	L	+76	$\bar{1}\bar{1}$,0,2	L	−78
804	B	+102	304	B	+65
$\bar{7}03$	L	−54			

ing that the product $F(h_1 k_1 l_1) \times F(h_2 k_2 l_2)$ determines the intensity of the secondary reflection it may be decided which pair is the most important one. With the exception of 500, and to some extent $\bar{1}\bar{1}$,0,2 also, the agreement is quite satisfactory. Since the Borrmann fan in the dynamical theory obeys Bragg's equation approximately, the deviation for 500 is astonishing. One possible explanation might be that the list of exciting primary reflections is not complete. In fact, there are many other weaker primary reflections observed and even the weaker ones may be involved if the secondary ones belong to the group of strong reflections. Surprisingly, from Table 2, the secondary reflections $\bar{1}\bar{1}$,0,2, 304, and $\bar{7}03$ should be excited by the group 210, $2\bar{1}0$; 310, $3\bar{1}0$ or $\bar{2}10$, $\bar{2}\bar{1}0$; $\bar{3}10$, $3\bar{1}0$. A comparison of their angular positions in Tables 1 and 2 (x^*, z^*) shows clearly that $\bar{1}\bar{1}$,0,2 especially does not satisfy the diffraction condition of the kinematic theory. This holds for the angle at the point of the arrow ψ' as well. Apparently, the same is true for 500 and $\bar{5}00$.

Let us now discuss a 'normal' diffraction pattern given for the reflection 802 in Fig. 7(*a*). The diffraction scheme is given in Table 4. In the direction $\mathbf{s}_3$ where the primary reflection 802 is observed the secondary reflections occur, generated by the primary reflections $42\bar{1}$ and 421, which are both very strong. Obviously, the lower wing represents the first, and the upper wing the second one. In the overlapping area of both, the focused primary reflection 802 is observed with very high intensity, although 802 belongs to the group of weak reflections of α-phenazine. As indicated in Table 3, nearly all reflections involved belong to the Laue case. Hence, the primary wave fields propagate into the interior of the crystal (the fluctuation in intensity is due to the mosaic structure of $K11$). Fig. 7(*b*) shows the same reflection of $K11$ in a photograph where the

crystal is rotated by 0·5° approximately, such that 804 is now primarily excited, but it can clearly be seen that 804 is again accompanied by secondary reflections, which apparently (angle ψ') are excited by 310 (and 210 probably), although there is a clear deviation from the Ewald sphere. Since 804 (primary reflection) belongs to the Bragg case (*cf.* Table 3), the generation of the primary and secondary beam is different! In spite of this, the focusing condition for the primary reflection is satisfied (as demonstrated in Fig. 1*a*). We get a (very weak) primary reflection, while the secondary one is now a single wing, represented by two diffraction lines. The asymmetric behaviour is due to a slight misadjustment of the crystal. This indicates clearly that the boundary conditions play an important role in the propagation of the wave fields in question. Although Table 2 tells us that only one reflection, namely 421, has sufficient intensity to be a possible partner to generate 802, the secondary reflection again is very sensitive to the slight misadjustment of the crystal. It will be shown later that this effect could be explained by an incomplete Borrmann fan, which may happen when the conditions for multiple scattering are met inadequately.

Table 4. *Diffraction scheme of primary and secondary reflections in the four-beam case* 802

Exciting beam	$\mathbf{s}_0$	$\mathbf{s}_1$	$\mathbf{s}_2$	$\mathbf{s}_3$
Diffracted beam				
$\mathbf{s}_0$	—	$\bar{4}\bar{2}\bar{1}$	$\bar{4}2\bar{1}$	$\bar{8}0\bar{2}$
$\mathbf{s}_1$	421	—	040	$\bar{4}2\bar{1}$
$\mathbf{s}_2$	$4\bar{2}1$	$0\bar{4}0$	—	$\bar{4}\bar{2}\bar{1}$
$\mathbf{s}_3$	802	$4\bar{2}1$	421	—

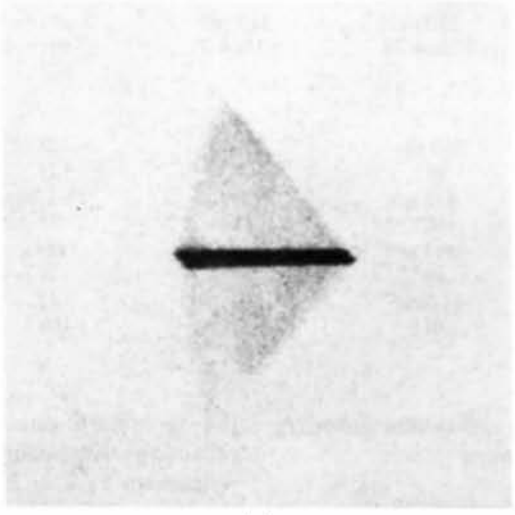

(*a*)

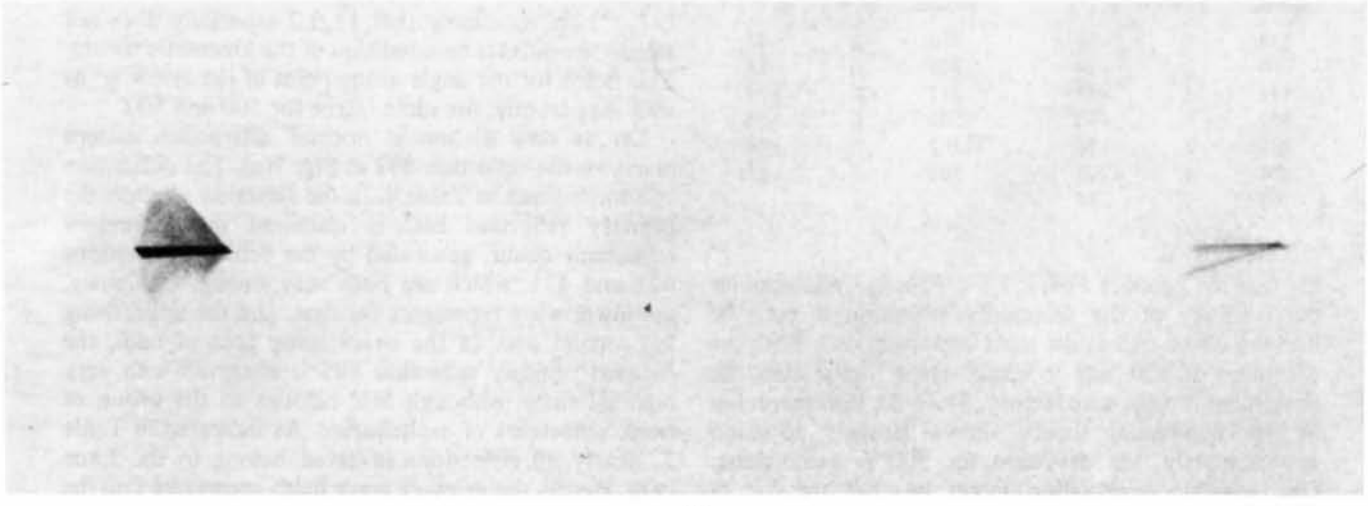

(*b*)

Fig. 7. Secondary reflections *h*0*l* in cases where the primary beam is not absent, *h*0*l* with $h = 2n$ ($K11$). (*a*) 802. Magnification 20 ×. (*b*) 804 and 802 (0·5° off optimal position). Magnification 10×.

Fig. 8(*a*), (*b*), shows the extinguished reflection $\bar{1}\bar{1},0,2$ for a very perfect crystal, *K*9 (8*a*), and the imperfect crystal *K*11 (8*b*). Both pictures are taken with the same magnification (20×). No focused primary reflection may be detected, indicating that the extinction rule is strictly obeyed in α-phenazine. Again, the two wings of the Borrmann fan are clearly seen, but there are apparently interference effects on them and a small, bright line is visible between the two wings. In the kinematic approximation this bright line may be explained as follows. According to Table 2 the most probable pairs generating the secondary reflections $\bar{1}\bar{1},0,2$ are $\bar{3}10$, $\bar{8}\bar{1}2$ and $3\bar{1}0$, $8\bar{1}2$ (upper and lower wing, respectively). According to the symmetry of the space group

$$F(hkl) = F(h\bar{k}l) \quad \text{if } h + k = 2n,$$
$$F(hkl) = -F(h\bar{k}l) \quad \text{if } h + k = 2n + 1.$$

Therefore, $\bar{3}10$ and $\bar{3}\bar{1}0$ have the same, but $\bar{8}\bar{1}2$ and $\bar{8}12$ opposite signs. Consequently, the two secondary reflections have opposite signs and should be extinguished in the overlapping area of propagation. Since both pairs belong to the same generation of wave fields, this condition should be valid in the dynamical theory as well. In the kinematic approximation a primary and secondary wave field cannot interfere because of the very low amplitude of the secondary wave field when compared with the primary one (exception: primary waves almost extinguished). Consequently, it may well be understood that the bright line is rather insensitive to

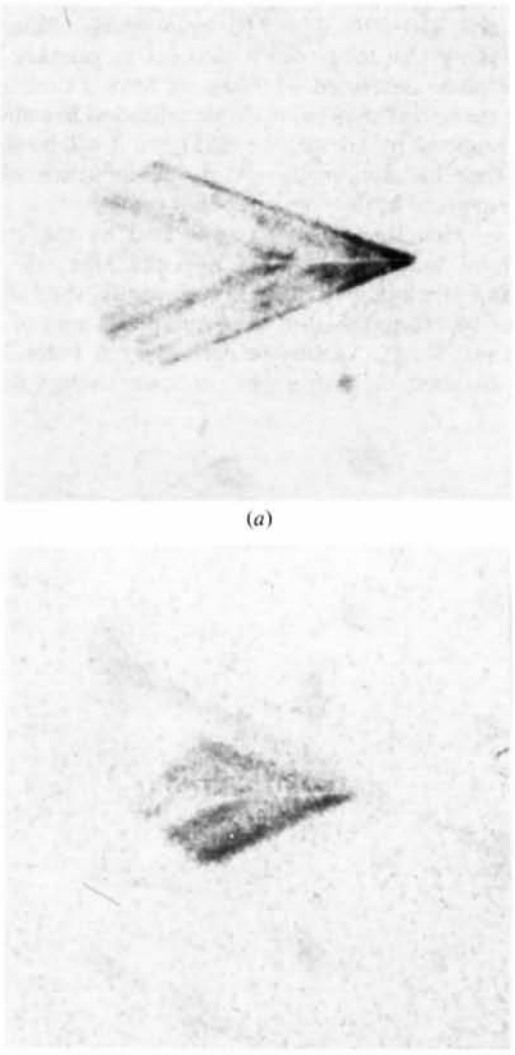

(*a*)

(*b*)

Fig. 8. Secondary reflections $\bar{1}\bar{1},0,2$, primary reflection absent ($h = 2n + 1$). (*a*) *K*9 (mosaic spread is small). (*b*) *K*11 (medium mosaic spread). Magnification 20×.

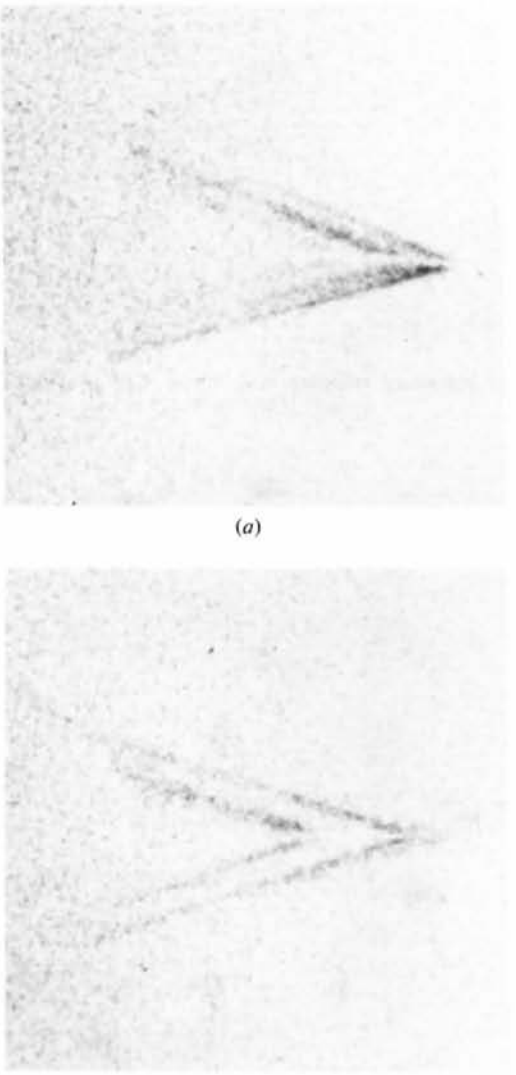

(*a*)

(*b*)

Fig. 9. Secondary reflections 304 for crystal *K*9 (perfect). (*a*) Optimal setting. (*b*) Rotated by 0·5° off optimal setting. Magnification 20×.

the mosaic spread which apparently is much larger in $K11$. It should be noted that the thickness of the plate (001) $K11$ was about half the thickness of the perfect crystal $K9$.

Fig. 9 shows a pair of secondary reflections 304 of the perfect crystal $K9$. The primary reflection 304 (Bragg case) is extinguished. The similarity of the $\bar{1}\bar{1}$,0,2 and 304 is striking, indicating that our effect is of much more general validity than expected. Fig. 9(*b*) shows the same bright line as Fig. 9(*a*), but again the interference picture of the wings is sensitive to the angular setting. It should be pointed out that the bright line in the overlapping range of the two wings may be detected in $K11$ too. Finally, Fig. 10 shows the reflection $\bar{7}03$ with a similarly close agreement with 304 and $\bar{1}\bar{1}$,0,2. The crystal $K14$ used for this picture had a mosaic spread between those of $K9$ and $K11$.

Fig. 10. Secondary reflection $\bar{7}03$, crystal $K14$ (medium mosaic spread). Magnification 20×.

4. Reflections 500 and $\bar{5}00$

The secondary reflections 500 and $\bar{5}00$ show very unusual behavior as has already been concluded from Table 2, where it has been pointed out that the theoretical angle ψ' at the head of the arrow was not realized, although there is no doubt that this most intense pair is generated by the four pairs 210 $3\bar{1}0$, 310 $2\bar{1}0$, and $3\bar{1}0$ 210, $2\bar{1}0$ 310, respectively. Since the secondarily reflecting planes also act as primary ones (situation as described for 802), we have a similar six-beam case. This unusual multiple reflection has already been reported by Hirshfeld (1955), but it will be shown here that his arguments about the influence of the mosaic spread of the crystal are not proved.

Each wing is now being generated by the contribution of two pairs having opposite signs of their resulting amplitude (Fig. 6); consequently, they should at least be extinguished in the overlapping area of each of the two wings. As may be derived from Table 2, the angle between the two upper (or lower) wings should

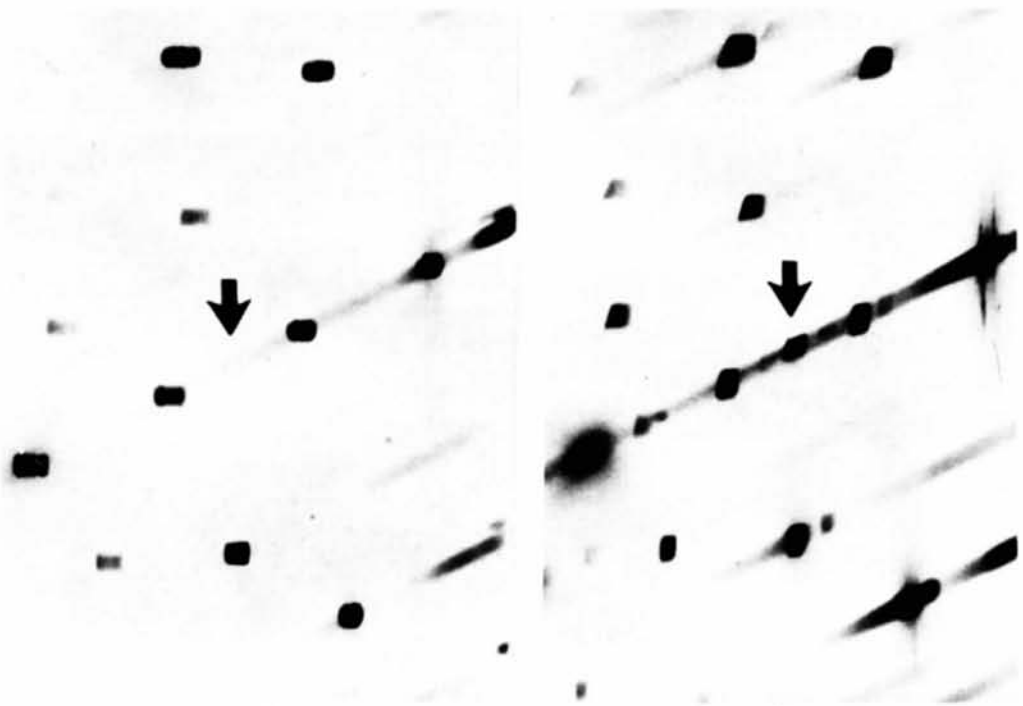

(*a*) (*b*)

Fig. 11. Weissenberg pictures of 500 reflections. (*a*) $K9$ (perfect). (*b*) $K4$ (imperfect).

differ by about 20°, this angular deviation should be observable. We have very carefully checked the numerous photographs available, but no such overlapping effect between two wings could be detected even in crystals with a large mosaic spread. Thus, we have either to conclude that both primary beams form a single wave field in the interior of the crystal or only one reflection contributes to it. Since the kinematic solution of the diffraction problem tells us that either both 310 and 210 or none of them meet the Ewald sphere simultaneously with 500, it is most probable that both of them contribute to the multiple diffraction. So why does the common wave field show no complete extinction? The reader will easily verify from the discussion above that even in a mosaic block both waves should be extinguished by interference. Hence, the only possible explanation for the strong enhancement of the 500 reflection with increasing mosaic spread could be given by assuming that the diffraction condition of multiple scattering is obeyed only approximately. Furthermore, we started with the erroneous assumption that the wave field may be represented by a single plane wave, but this naturally does not hold for the primary and secondary wave dying out in a thick crystal because of their contributions to the total wave field becoming increasingly 'small' with increasing length of their path within the crystal. Deviations from the exact Bragg condition result in phase changes of the spherical waves, hence, interference patterns are possible. Therefore, the interference phenomena may be changed as pointed out above; it is not clear whether the excitation conditions to be determined by constructing the complicated system of dispersion surfaces are really satisfied. If they are not, then the excitation in a very perfect crystal does not take place, but it certainly does so in an imperfect one as an incoherent scattering

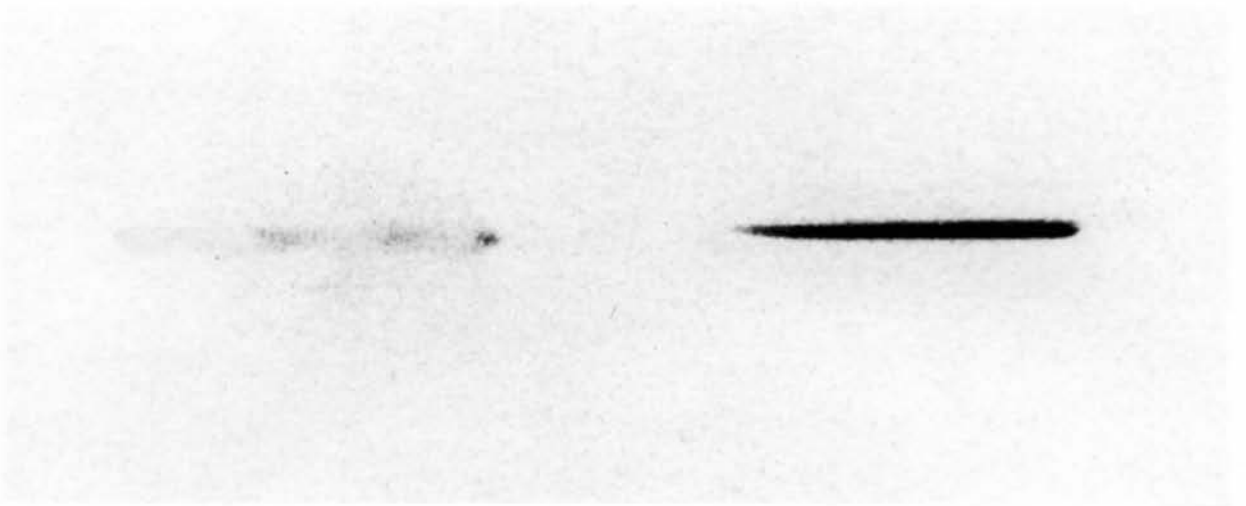

(*a*)

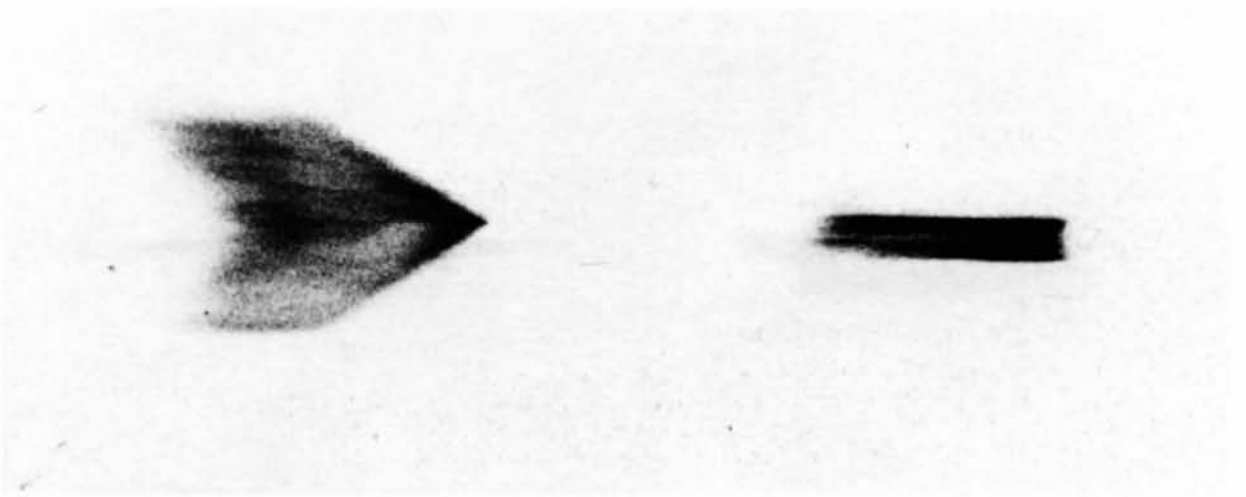

(*b*)

Fig. 12. 10° oscillation strictly monochromatic and focused. (*a*) *K*9 (perfect). (*b*) *K*4 (imperfect) ($\psi' \simeq 70°$!). Magnification 20×.

process. For this reason we cannot expect that 500 gives a diffraction pattern which can easily be interpreted. That this assumption may be correct can be derived from Fig. 11, where the part of a Weissenberg pattern relevant for the 500 secondary reflection is shown for two different crystals: one of them is our most perfect crystal $K9$, showing no sign of the secondary reflection, while the second picture is taken with the very imperfect crystal $K4$, showing that the secondary 500 is comparable in intensity with primary reflections of medium intensity. A comparison between Figs. 8 and 11 clearly reveals the difference in the influence of the mosaic structure. $\bar{1}\bar{1}$,0,2 is nearly uninfluenced since the same approximate exposure time was allowed for both pictures. The big difference in the intensity of the 500 reflection is demonstrated once more in Fig. 12, showing a 10° oscillation picture for the very perfect crystal $K9$ and the imperfect one $K4$. It should be noted that the secondary reflection is not affected (point of the arrowhead sharp) by the condition of focusing, which is not satisfactory in the case of the $K4$ diffraction picture. Two diffraction pictures of 500 and $\bar{5}00$ of the same crystal, $K11$, in Fig. 13, show very distinctly that the shape of the two spots is different, even in the case of a certain mosaic spread. This has nothing to do with the invalidity of Friedel's law, it is just a consequence of the two physically different situations for reflecting the group 500 and $\bar{5}00$, generated by rotating the Ewald sphere by 37°.

The big difference in the propagation of waves within the crystal is shown in a series of pictures taken by the Noromosic technique. Each one of them differs by a rotation of 0·5°. The large azimuthal angle prevents important information of the diffraction pattern being lost. The three crystals, $K9$ (perfect), $K10$ (less perfect)

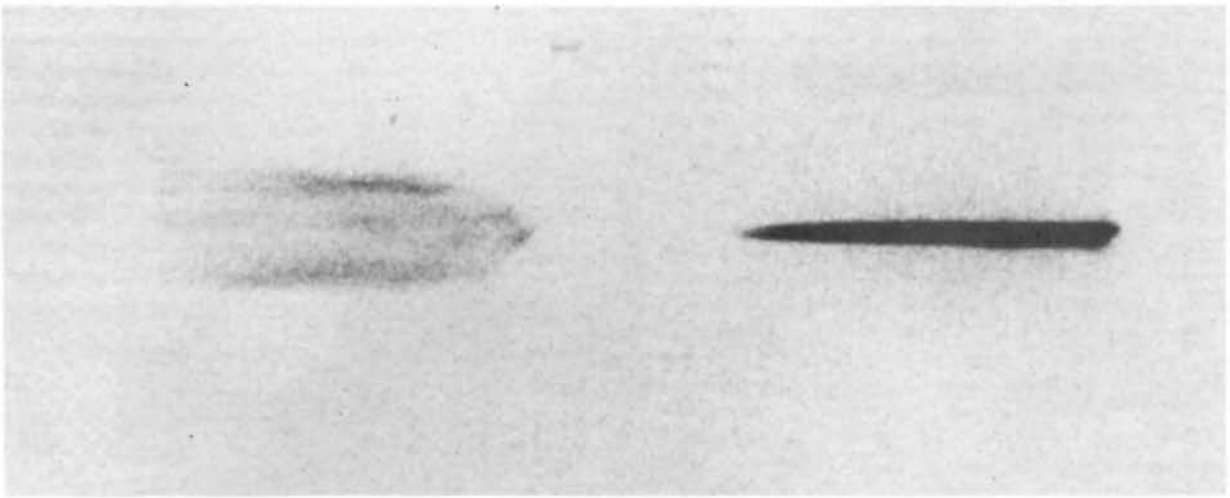

(*a*)

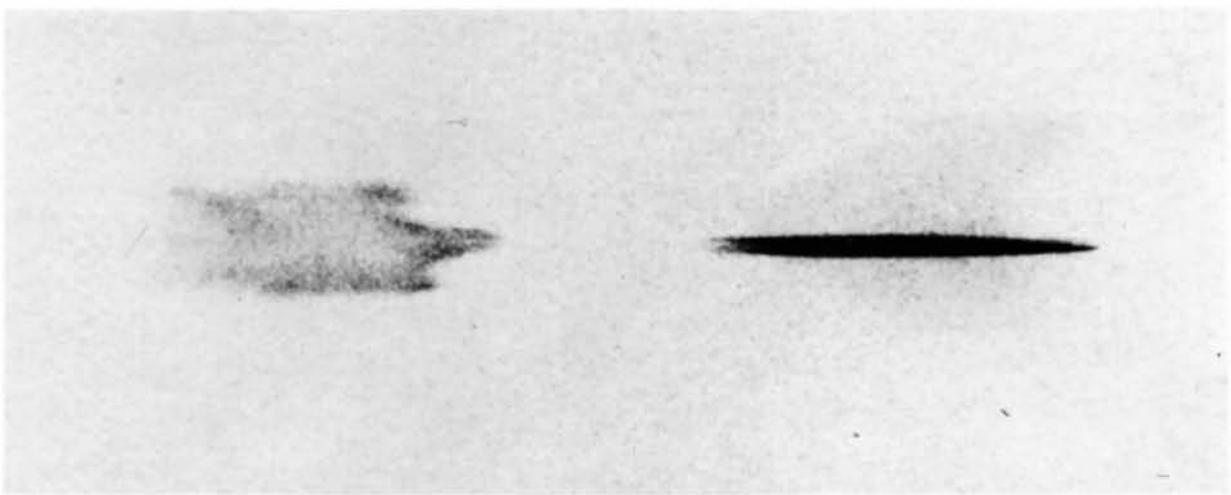

(*b*)

Fig. 13. 10° oscillation picture (compare with Fig. 12) of $K11$. (*a*) $\bar{5}00$ and $\bar{6}00$. (*b*) 500 and 600. Magnification 20×.

and $K11$ (rather imperfect), clearly show that these interference effects are sensitive to the mosaic structure of the crystals. Fig. 14(*a*), (*b*) shows pictures of the $\bar{5}00$ reflection, while Fig. 14(*c*) shows the 500 reflection. It should be pointed out that $\bar{5}00$ of $K14$ was not very different from the one given in Fig. 14(*b*), therefore it has been omitted here. The physically different diffraction for $\bar{5}00$ and 500 may easily be seen. This is again

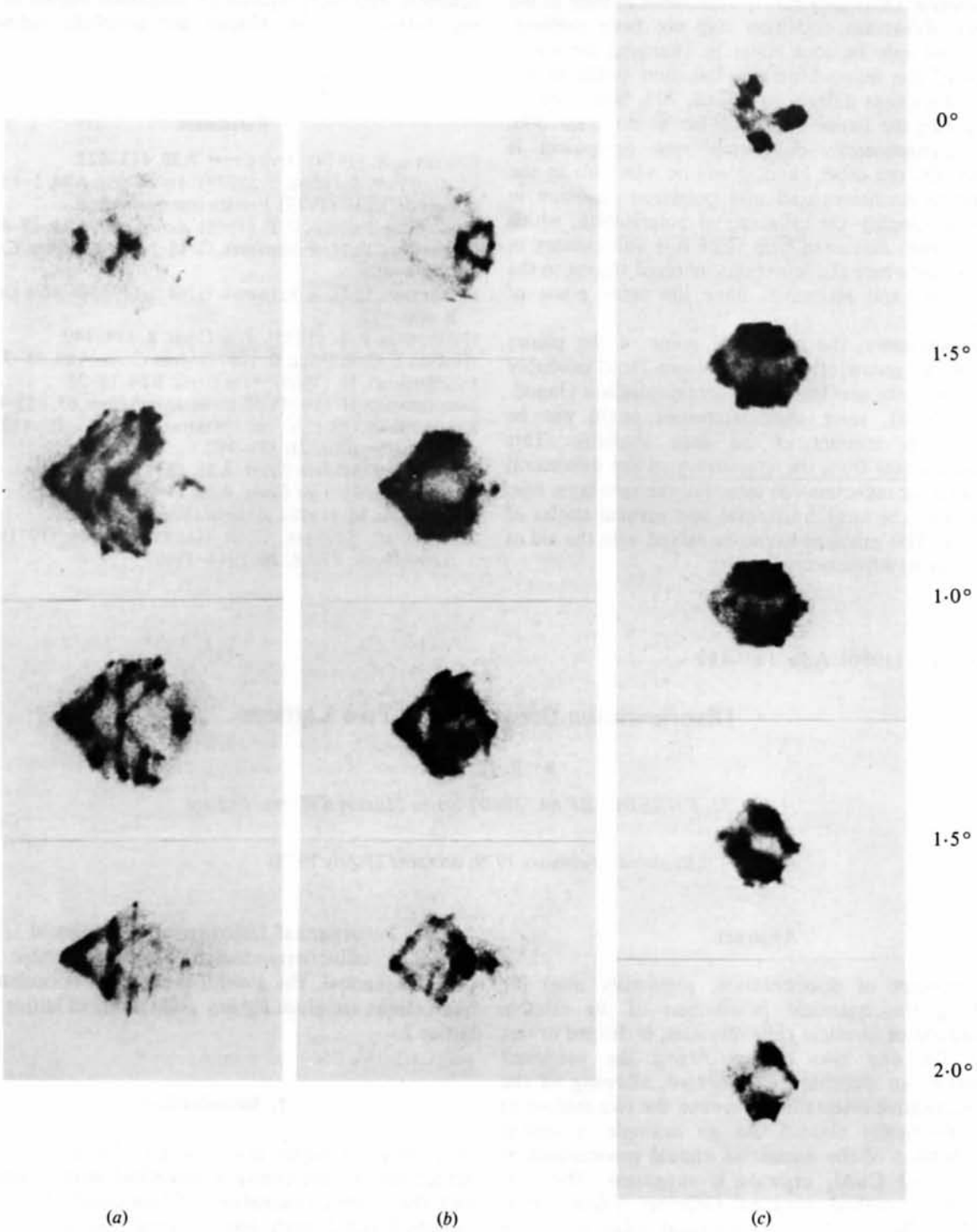

Fig. 14. Series of photographs in the Noromosic technique differing by 0·5° angular setting. (*a*) $K9$, $\bar{5}00$ (perfect). (*b*) K 10, $\bar{5}00$ (medium quality). (*c*) $K11$, 500 (medium). Magnification 18×.

supported by the oscillation picture showing $\bar{5}00$ and 500 in Fig. 13.

No attempt will be made in this paper to give a full theoretical interpretation of the various diffraction phenomena. Obviously this is impossible as long as the correct diffraction condition has not been realized, which can only be done either by changing the wavelength of the monochromatic radiation (valid in the cases of multiple diffraction $\bar{1}\bar{1}$,0,2, $\bar{7}03$, 804, 304), or by varying the lattice constants (to be done for 500, 802). Consequently, completely new equipment is needed. On the other hand, it will be advisable to use strictly monochromatized and polarized radiation in order to simplify the influence of polarization, which has not been discussed here since it is unnecessary in those cases where the reflections involved belong to the same zone and all waves have the same plane of incidence.

Unfortunately, the indices of some of the planes relevant to secondary reflections are most probably incorrect in the previous short communication (Jagodzinski, 1978), since their intensities could not be checked on account of the data available. This difficulty arises from the inaccuracy of the diffraction condition for reflections on other but the zero layer line, because of the large horizontal and vertical angles of aperture. This problem has to be solved with the aid of more precise diffraction geometry.

The author thanks the Deutsche Forschungsgemeinschaft for generously supplying X-ray equipment. Technical assistance in taking and evaluating diffraction pictures by Mrs Oppermann and Mrs Schmidt, and reproduction of magnified copies of X-ray patterns by Mr Gappa are gratefully acknowledged.

References

COLLELA, R. (1974). *Acta Cryst.* A**30**, 413–423.
EWALD, P. P. & HÉNO, Y. (1968). *Acta Cryst.* A**24**, 5–15.
HAUSSER, K. H. (1979). Private communication.
HÉNO, Y. & EWALD, P. P. (1968). *Acta Cryst.* A**24**, 16–42.
HERBSTEIN, F. H. & SCHMIDT, G. M. J. (1955*a*). *Acta Cryst.* **8**, 399–405.
HERBSTEIN, F. H. & SCHMIDT, G. M. J. (1955*b*). *Acta Cryst.* **8**, 406–412.
HIRSHFELD, F. L. (1955). *Acta Cryst.* **8**, 439–440.
HUANG, T. C. & POST, B. (1973). *Acta Cryst.* A**29**, 35–37.
JAGODZINSKI, H. (1968). *Acta Cryst.* B**24**, 19–23.
JAGODZINSKI, H. (1978). *Naturwissenschaften*, **65**, 651–652.
KSHEVETSKY, S. A. & MIKHAILYUK, I. P. (1976). *Kristallografiya*, **21**, 381–382.
POST, B. (1975). *Acta Cryst.* A**31**, 153–155.
POST, B. (1979). *Acta Cryst.* A**35**, 17–21.
RENNINGER, M. (1978). *Z. Kristallogr.* **147**, 5–11.
SCHUCH, H., STEHLIK, D. & HAUSSER, K. H. (1971). *Z. Naturforsch. Teil A*, **26**, 1944–1969.

Acta Cryst. (1980). A**36**, 116–122

Disorientation Between Any Two Lattices

BY R. BONNET

LTPCM, ENSEEG, BP 44, 38401 *Saint Martin d'Hères, France*

(*Received* 9 *February* 1979; *accepted* 25 *July* 1979)

Abstract

The concept of disorientation, previously used for studying the statistical distribution of the relative orientation of identical cubic crystals, is defined in this work for any two lattices. Using the proposed definition, an algorithm is presented, allowing all the known relative orientations between the two lattices to be conveniently classed. As an example, a unified classification of the numerous mutual orientations of the Al and $CuAl_2$ crystals is suggested. The unit quaternion method used by Grimmer [*Acta Cryst.* (1974), A**30**, 685–688] for identical cubic lattices is here proved efficient for discussing the pair axis/angle disorientations in more complicated cases: cubic 1/cubic 2; tetragonal 1/tetragonal 2; hexagonal 1/hexagonal 2; cubic/tetragonal; cubic/orthorhombic and cubic/hexagonal. The general expressions of equivalent quaternions are given for any point group of lattice 1 or lattice 2.

1. Introduction

In a preceding paper, Bonnet & Cousineau (1977) presented results concerning a numerical method used to find the relative orientations of two equal or different lattices 1 and 2, such that two small multiple cells $M1$ and $M2$ are coincident or near-coincident to within a small deformation. Their results were classified in

0567-7394/80/010116-07$01.00